ELSEVIER

Solid State Ionics 152–153 (2002) 181–188

SOLID STATE IONICS

www.elsevier.com/locate/ssi

Structure-related intercalation behaviour of $LiCoO_2$ films

P.J. Bouwman [a,*], B.A. Boukamp [a], H.J.M. Bouwmeester [a], P.H.L. Notten [b]

[a] *Laboratory of Inorganic Materials Science, Faculty of Chemical Technology and MESA+ Research Institute, University of Twente, PO Box 217, 7500 AE Enschede, The Netherlands*

[b] *Philips Research Laboratory, Professor Holstlaan 4, 5656 AA Eindhoven, The Netherlands*

Accepted 14 February 2002

Abstract

Submicron films of $LiCoO_2$ have been deposited on silicon and stainless steel substrates using RF sputtering and pulsed laser deposition (PLD). Both films show preferred orientation. RF films have their Li diffusion plane oriented favourably, that is, perpendicular to the surface, while PLD films show a parallel, *c*-axis orientation. Electrochemical experiments indicate a strong dependence of the intercalation rate on the alignment of the host structure toward the electrolyte solution. Lithographic patterning enhances the inferior intercalation properties of the PLD film on silicon, as does the utilisation of stainless steel substrates.

Keywords: Thin film; $LiCoO_2$; Intercalation; Preferential orientation

1. Introduction

The high cycling stability of $LiCoO_2$ and its high cell potential against lithium makes it an attractive intercalation electrode for micro-scale power supplies.

The layered $LiCoO_2$ intercalation host can be derived from the rocksalt structure. The structure is rhombohedral (space group $R\bar{3}m$) with cobalt and lithium alternately occupying octahedral sites between adjacent close-packed planes of oxygen. Approximately half of the lithium can reversibly be extracted and re-inserted electrochemically, before any structural degradation occurs. Diffusion of lithium proceeds through a vacancy hopping mechanism within the lithium plane and is thus strictly two-dimensional.

Oriented submicron $LiCoO_2$ films have been deposited on conducting silicon substrates [1]. The preferential orientation of the polycrystalline films depends on the conditions during deposition. The (00ℓ) orientation is obtained using the pulsed laser deposition (PLD) technique, while the (110) orientation is achieved with RF sputtering. Typical X-ray diffraction (XRD) patterns of both films with the different alignment relative to the substrate are shown in Fig. 1.

In this paper, the electrochemical intercalation properties of the oriented $LiCoO_2$ films are presented. RF films are expected to have a superior intercalation rate, due to their orientation of the lithium diffusion plane being directed toward the electrolyte solution, compared with the PLD films which have their diffusion plane oriented parallel with the electrolyte interface. The electrochemical performance of the latter films can possibly be improved with the introduction of pinholes and defects, which expose the underlying lithium diffusion planes.

* Corresponding author. Tel.: +31-53-489-2998; fax: +31-53-489-4683.

E-mail address: p.j.bouwman@ct.utwente.nl (P.J. Bouwman).

URL: http://ims.ct.utwente.nl.

0167-2738/02/$ - see front matter
PII: S0167-2738(02)00298-9

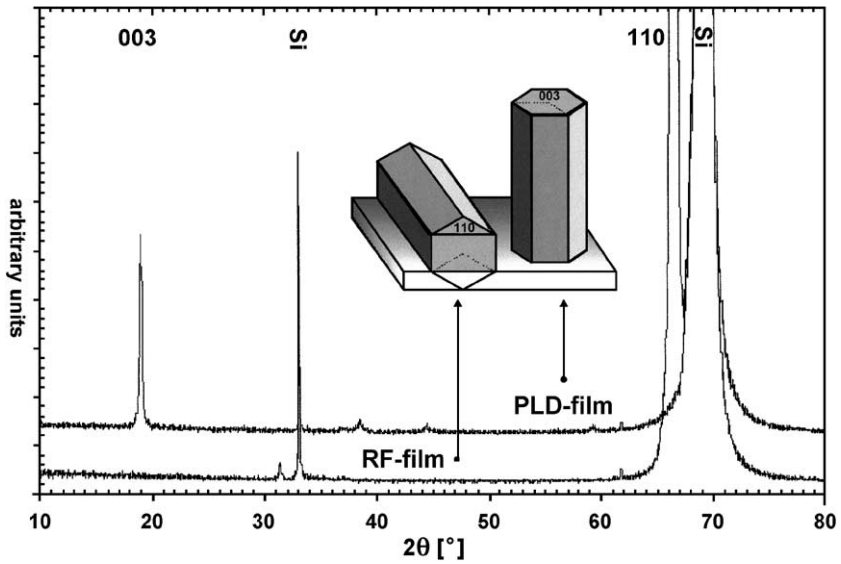

Fig. 1. XRD spectra of a typical RF and PLD films deposited on silicon and subsequently annealed at 600 °C for 30 min. The inset shows the orientation of the $LiCoO_2$ unit cell on the substrate surface.

The electrochemical properties of the $LiCoO_2$ films deposited on silicon substrates are compared with those of similar films deposited on polished stainless steel substrates. While exhibiting *c*-axis orientation, the films on metallic substrates are reported to have reasonable intercalation behaviour [2–4]. The influence of the substrate on the electrochemical properties of the film is analysed. The model describing the observed electrochemical behaviour will be presented in a future publication.

2. Experimental

2.1. Thin film deposition

Submicron $LiCoO_2$ films were prepared on stainless steel and silicon substrates with pulsed laser deposition and RF sputtering using stoichiometric $LiCoO_2$ targets. The metal substrate discs (15 mm ∅) were stamped from sheet metal and polished with diamond paste (1 μm). The silicon substrates (15 mm ∅) were doped with phosphor to obtain n-type electrical conductivity. For the deposition parameters used with RF sputtering and pulsed laser deposition, we refer to previously published work [1]. Annealing was either performed in situ in the vacuum chamber (pO_2=0.2 mbar) by increasing the substrate holder temperature or ex situ in a constant gas flow of 30 ml min^{-1} STP containing 90% O_2/10% N_2. The typical annealing process was 30 min at 600 °C using a ramp rate of 5 °C min^{-1} (in situ) or 2 °C min^{-1} (ex situ).

2.2. Structural analysis

The crystal structure of the submicron films was analysed with XRD using CuK_α at room temperature with a Philips PW 1800 diffractometer fitted with a rotating sample holder and an automatic divergence slit. Visualisation of the film surface morphology was performed using a JEOL JSM 5800 scanning electron microscope.

2.3. Electrochemical analysis

Electrochemical experiments were conducted with a PGstat20 Autolab Potentiostat (ECO-Chemie) using an integrated Frequency Response Analyser. The electrochemical cell comprised two electrodes: a met-

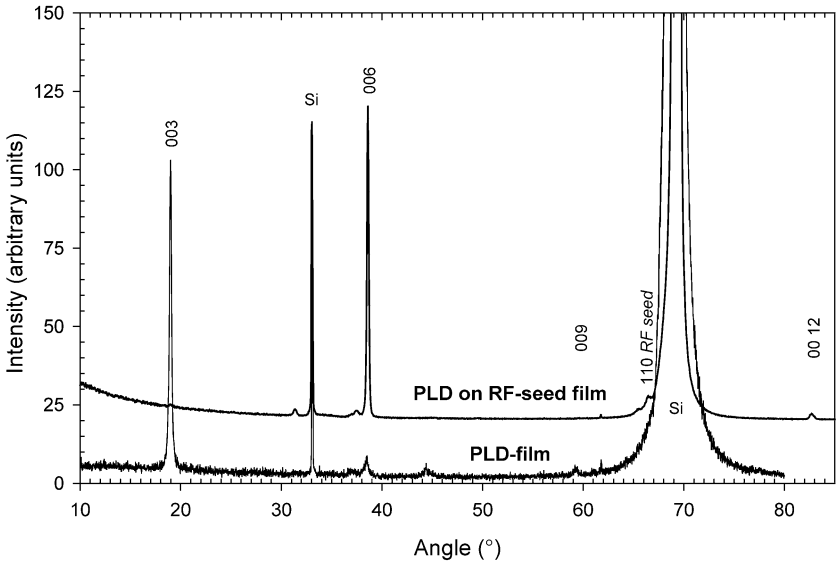

Fig. 2. XRD spectra of two, in situ annealed PLD films deposited simultaneously on a 0.1-μm RF-seed layer on silicon and on a blank silicon substrate, respectively.

allic lithium counter electrode and a working electrode. The electrodes were separated by a polymer sheet, which was soaked with commercial battery grade liquid electrolyte (1 M $LiClO_4$, EC:DEC 1:1, Merck). The cells were maintained and operated inside a helium glove box.

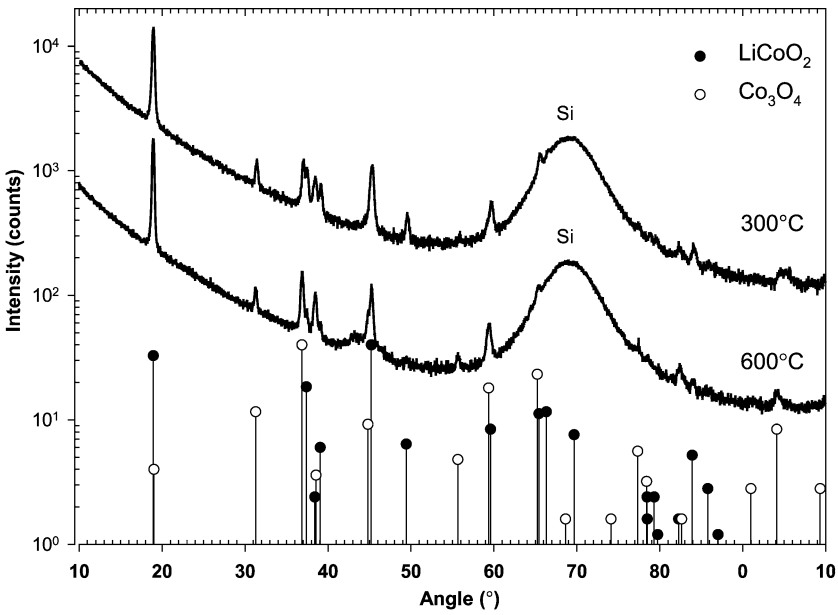

Fig. 3. XRD diagrams of a PLD film on silicon deposited at 300 °C and annealed in situ and a PLD film grown directly at 600 °C on silicon. The reference spectra of $LiCoO_2$ and Co_3O_4 are plotted as bars with closed and open circles, respectively. The intensity is plotted logarithmically to bring out the weak reflections.

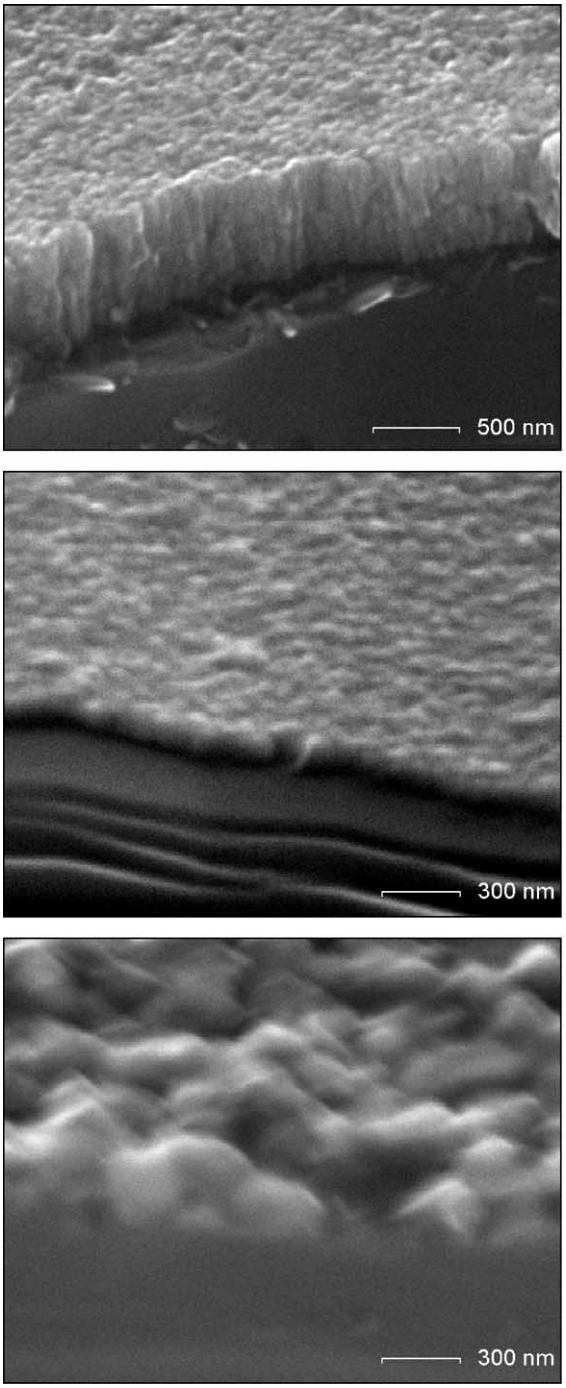

Fig. 4. SEM photographs of the $LiCoO_2$ films cross section on silicon substrate. Top: 0.5 μm RF film; centre: PLD film deposited at 300 °C and in situ annealed at 600 °C; bottom: PLD film deposited at 600 °C substrate temperature.

2.4. Lithographic patterning

In some PLD films, square islands of 0.1 mm^2 were bared at 0.1 mm spacing using standard lithographic techniques. These were etched with 5% HF solution leaving a gauze-like pattern in the $LiCoO_2$ film. One quarter of the active material was removed. These etched samples are referred to as 'patterned' films.

3. Results

Fig. 1 reveals the structure of the RF and PLD films commonly produced under the described deposition conditions on silicon substrates. In a separate experiment, a PLD film was simultaneously grown on a blank silicon substrate and on a silicon substrate covered previously with an RF-sputtered seed layer of 0.1 μm $LiCoO_2$ (annealed at 600 °C, 30 min) at 300 °C substrate temperature. Fig. 2 shows the XRD diagram of both samples after in situ annealing at 600 °C for 30 min. The reference sample reveals the typical PLD film diffraction pattern, indicating (00ℓ) lattice plane orientation. The PLD film deposited on the seed layer, which before the deposition experiment showed only the (110) reflection, now shows distinct (006) and (0012) reflections. The (00ℓ) orientation is maintained, but the (003) and (009) reflections are completely absent.

Fig. 3 shows the XRD patterns of two PLD films produced with an identical number of laser pulses.

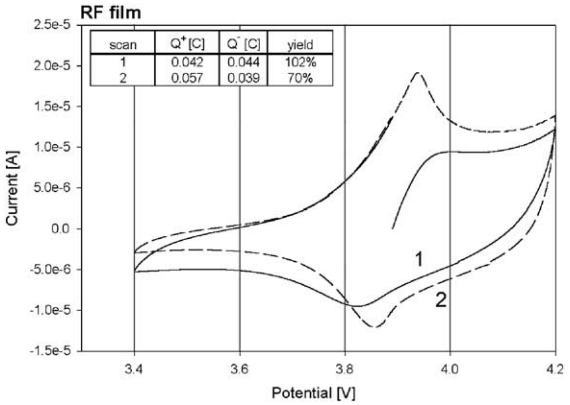

Fig. 5. Cyclic voltammogram of a 0.1-μm RF film recorded at 0.1 mV/s scan rate against metallic lithium. The capacity and yield of the first and second scan are noted in the inset table.

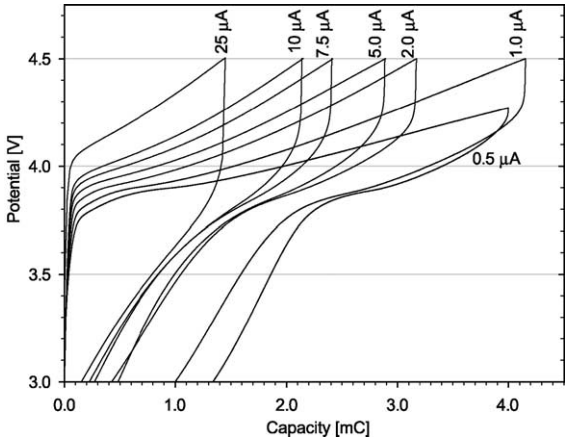

Fig. 6. Constant current charge–discharge diagram showing the cycling behaviour of a patterned PLD film at various currents between the cut-off voltages of 3.0 and 4.5 V.

The first is deposited at 300 °C and subsequently annealed at 600 °C (in situ) and the second grown directly at 600 °C. The intensity is plotted logarithmically to bring out the smaller diffraction peaks. Both samples exhibit a similar (00ℓ) orientation of the $LiCoO_2$. The sample grown at high substrate temperature generally shows increased Co_3O_4 diffraction intensity (only the peak at 31.2° remains similar).

The SEM pictures in Fig. 4 show the film topography of these samples. The photograph of an annealed 0.5-µm RF film on silicon substrate is shown for comparison. Compared to the PLD film deposited at 300 °C, the film grown directly at 600 °C exhibits larger and non-uniform grains. Note, that the quantity of deposited $LiCoO_2$ matter is equal for both PLD films.

A cyclic voltammogram of a typical RF film recorded with a scan rate of 0.1 mV s^{-1} is shown in Fig. 5. The oxidation and reduction peaks become well defined upon the second cycle and are located at 3.94 and 3.86 V, respectively. The 84-mV peak separation is close to the 69 mV predicted by the Nernst equation, which is indicative of a good reversibility of the intercalation reaction. The capacity regained on discharge is close to the theoretical value of 48 mC (0.1 µm, 1.76 cm^2). The Faradaic yield decreases with subsequent cycles due to electrolyte decomposition at high electrode potentials. The PLD films deposited on silicon employ only 3% of their theoretical capacity, when subjected to cyclic voltammetry at this scan rate.

Fig. 6 shows the constant current charge and discharge behaviour of a patterned PLD film as a function of charge. The observed capacity accounts

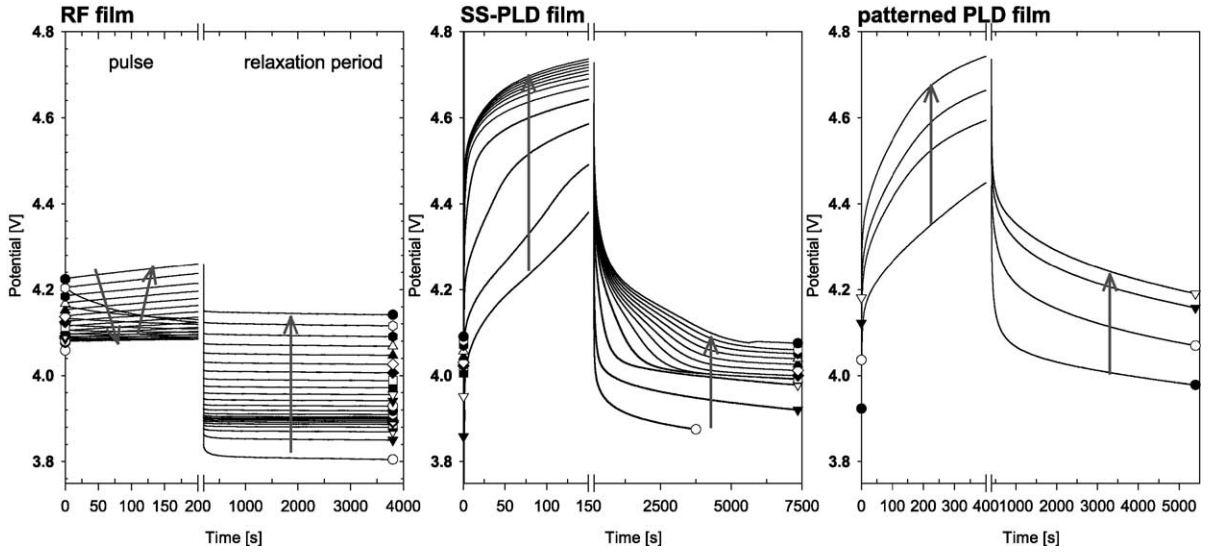

Fig. 7. Potential response to pulsed galvanostatic charging of an RF film, a PLD film on stainless steel substrate and a patterned PLD film on silicon as a function of time. The current pulse is followed by a period of zero-current relaxation before the next pulse is applied (arrows indicate pulse sequence).

for approximately 15% of the deposited $LiCoO_2$. This is an improvement on the untreated PLD films, where only 3–5% of the host material is involved in the intercalation process. Patterning of the PLD film results in a decrease of the overpotential and thus allows (dis-)charging with 10 μA or even 25 μA without immediately exceeding the cut-off voltages of 3.0 and 4.5 V. The maximum reversible capacity is observed with a cycling current of 1 μA. The irreversible capacity increases with lower currents due to the parasitic effect of the leakage current.

The potential response of various thin film electrodes to pulsed charging has been investigated. In Fig. 7, the results are shown of a typical RF film on silicon, PLD film on stainless steel and the patterned PLD film on silicon. The RF film is charged with a 50-μA pulses of duration 200 s, followed by a zero-current relaxation period. The stainless steel PLD film is charged with 10 μA pulses of 150 s and the patterned silicon PLD film to 2.5 μA pulses of 400 s. It was not possible to use a similar pulse for all three samples due to the unequal rate capabilities. The potential relaxation subsequent to a current pulse appears immediate for the RF film, while the silicon PLD film potential relaxation progresses into a linear decay. The voltage of the PLD film deposited on stainless steel also exhibits gradual relaxation behaviour typical of PLD films, but after some time stabilises at a new equilibrium potential as the RF film does.

4. Discussion

The close-packed (00ℓ) planes of $LiCoO_2$ have the highest density and a low surface energy. These planes are preferentially formed parallel to the substrate surface in the kinetic growth regime at high deposition rates [5]. This orientation is observed for PLD films, which indeed have a high momentary growth rate due to the pulsed nature of the applied plasma. With increasing film thickness (>0.2 μm), the *c*-axis orientation is no longer stable and the preferential orientation of the PLD films gradually disappears.

The RF films are deposited with continuous plasma at low power, which results in an '*a*-axis' orientation of the $LiCoO_2$. Crystal growth occurs fastest in the *a*-axis direction and is here aligned normal to the substrate surface. This (110) alignment appears thermodynamically stable, since it is possible to grow thick RF films (>0.75 μm) without losing preferential orientation. The adverse (00ℓ) orientation reappears at increased RF-plasma deposition rate.

When $LiCoO_2$ is deposited by means of PLD on an annealed RF seed layer, the existing (110) orientation is not continued, but overgrown with a preferential (00ℓ) alignment. However, the film structure differs from that grown on a blank silicon substrate, as not all (00ℓ) reflections are observed. The distinctive diffraction pattern can be explained by assuming complete cationic disorder [6]. A random distribution of the lithium and cobalt ions leads to a structure similar to that of NaCl, which explains that the (003) and (009) reflections become extinct. The present results clearly demonstrate that the type of substrate affects the growth kinetics of the $LiCoO_2$ during PLD deposition.

The orientation of the layered intercalation host toward the electrolyte solution is of prime importance for the observed electrochemical intercalation behaviour. The two contrasting situations are visualised in Fig. 8. Lithium (de-)intercalation in an RF film

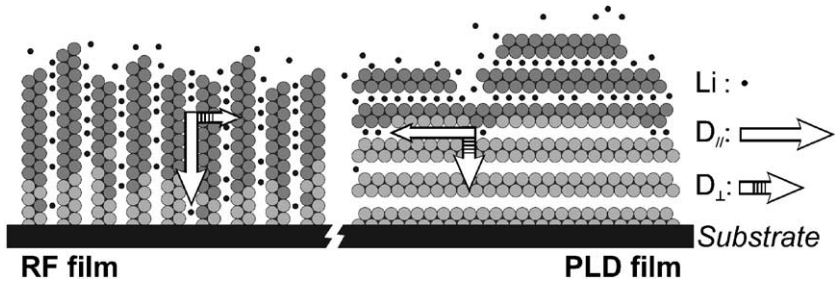

Fig. 8. Schematic representation of the lithium intercalation process in case of the RF film (left) and the PLD film (right). *D* represents the lithium diffusion parallel and $D_\perp$ the diffusion normal to the diffusion planes. The permanent lithium atoms are not drawn for clarity.

proceeds along the two-dimensional lithium diffusion plane, while in case of the PLD film, the overall intercalation direction is normal to these diffusion planes. Transport of lithium across the CoO_2 sandwiches is negligible, so lithium intercalation of the PLD film is highly dependent on other means of inward lithium transport (e.g. grain boundaries, defects, cracks).

Structural analysis shows that deposition of $LiCoO_2$ on silicon substrates and subsequent annealing treatment leads to polycrystalline films with a high degree of preferential orientation. Inhomogeneities due to grain growth are observed when the films are subjected to elevated temperatures (600 °C) for long periods of time (>30 min). Annealing treatment at this temperature also leads to evaporation of volatile Li_2O, which results in Co_3O_4 formation (estimated ~5% in Fig. 3). Annealing is unnecessary with direct film deposition at 600 °C. However, these films develop large, individual grains with dimensions ranging from 100 to 500 nm and an increased amount of Co_3O_4 due to the long deposition time (approximately 2 h). Although these irregular $LiCoO_2$ films show improved intercalation activity, their non-uniformity makes them unsuitable for fundamental research.

Patterning of the $LiCoO_2$ PLD film on silicon is an accurate technique to increase the exposure of the lithium diffusion planes. The intercalation rate of the RF film shows no gain from patterning, since the favourable host alignment already provides optimal exposure. The improvement of the PLD film intercalation properties is evident from the decreased overpotential during cycling between 3.0 and 4.5 V and the feasibility of currents as high as 25 μA. The reversible capacity of the PLD films generally increases with patterning from 3% to 15% of its theoretical capacity. The mesh of the gauze-like pattern remains large compared to the film thickness. Apparently not all the active material is 'accessible' from the electrolyte solution and thus capable of intercalation.

The microscopically rough surfaces of the polished stainless steel substrates are expected to introduce numerous defects in the deposited film. This coincides with the superior electrochemical behaviour observed for stainless steel PLD films compared to the regular and even the patterned PLD films on silicon substrates, considering intercalation rate and capacity. The current pulse response of the stainless steel PLD film appears to be combination of the RF film and the patterned PLD film on silicon. The high overpotential during the pulse and the slow potential relaxation afterwards is typical for PLD films. The continuous potential decay of the PLD films is caused by the limited intercalation rate connected to the slow internal lithium diffusion. The OCP stabilisation obtained after a specific relaxation period is typical for the RF films and also observed for PLD films on stainless steel substrates. It is assumed that the high degree of defects in the PLD film on stainless steel increases the diffusion plane exposure and decreases the lithium diffusion distance within the intercalation host. Thus, fast equilibration of the intercalated lithium concentration profile is achieved, analogous to the RF film behaviour. A similar effect could be realised for the patterned PLD films on silicon by etching a gauze-like pattern of (sub-)micron mesh dimensions.

The electrochemical intercalation process in the $LiCoO_2$ film is clearly controlled by the orientation of the two-dimensional diffusion plane toward the electrolyte solution. Defects and film irregularities only enhance the intercalation rate and capacity of a thin film electrode in case of an unfavourable (00ℓ) host orientation. The (110)-oriented RF films on silicon substrate remain the most suitable electrodes for future application in solid state devices.

5. Conclusions

The alignment of the two-dimensional diffusion plane to the electrolyte solution appears perpendicular (hence accessible) or parallel (thus inaccessible) in RF films and PLD film, respectively, and is related to the deposition circumstances. The large influence of the host orientation on the intercalation process is reflected by the electrochemical behaviour. The RF films utilise almost their full theoretical capacity during cycling at high current densities showing low overpotentials. This is in contrast with the PLD films, which show inferior reversible capacity at low current densities together with extreme overpotentials. In the latter case, the electrochemical properties may be improved by introducing defects and irregularities in the thin-film electrode. This is either achieved in an

uncontrolled manner through prolonged high-temperature treatment, film deposition on stainless steel substrates or accurately using lithographic patterning techniques. Still, the increased exposure of the diffusion plane through defect introduction cannot compensate for the adverse effect of its unfavourable alignment. The preparation of $LiCoO_2$ thin-film electrodes in the preferential (110) orientation (RF sputtering) is recommended for superior electrochemical intercalation performance.

Acknowledgements

This research was made possible due to financial support from FOM. The authors are indebted to Philips Research Laboratory for technical support on sample preparation and characterization. Special thanks are due to J.F.M. Cillessen for operation and assistance on the PLD equipment, H. Koster for the SEM analysis; the Philips CFT department for the XRD measurements.

References

[1] P.J. Bouwman, B.A. Boukamp, H.J.M. Bouwmeester, H.J. Wondergem, P.H.L. Notten, J. Electrochem. Soc. 148 (4) (2001) A311.
[2] P. Fragnaud, T. Brousse, D.M. Schleich, J. Power Sources 63 (1996) 187–191.
[3] K.A. Striebel, C.Z. Deng, S.J. Wen, E.J. Cairns, J. Electrochem. Soc. 143 (6) (1996) 1821.
[4] Y. Iriyama, M. Inaba, T. Abe, Z. Ogumi, J. Power Sources 94 (2001) 175.
[5] K. Nishioka, N. Mizutani, H. Komiyama, J. Electrochem. Soc. 147 (4) (2000) 1440.
[6] H.W. Wang, Y.I. Jang, B. Huang, D.R. Sadoway, Y.M. Chiang, J. Electrochem. Soc. 146 (1999) 473.